THE AMERICAN SOCIETY OF MECHANICAL ENGINEERS
345 E. 47 St., New York, N.Y. 10017

90-GT-80

The LCF Behavior of Several Solid Solution Strengthened Alloys Used in Gas Turbine Engines

S. K. SRIVASTAVA and D. L. KLARSTROM
Haynes International, Inc.
Kokomo, IN 46902-9013

ABSTRACT

LCF tests were performed on production plate (16mm thick) materials of HAYNES® alloy No. 230, HASTELLOY® alloy X and INCONEL® alloy 617. The tests were conducted in air at 760, 871 and 982°C under the fully reversed strain controlled mode on materials in the annealed condition. The results showed that 230™ alloy possesses the best low cycle fatigue characteristics followed by alloy X and alloy 617 under all test conditions. The paper presents total strain range-life data, cyclic hardening/softening, and metallographic observations on selected failed samples. It is shown that oxidation plays a key role in fatigue-crack initiation in alloy 617.

INTRODUCTION

Gas turbine engines are complex machines consisting of numerous components. Many of these components, such as combustor cans, liners, flame holders, ducts, seal rings, etc. are fabricated of solid solution strengthened wrought nickel-base superalloys. In service these components undergo cycling between idle and operating conditions and thus are subjected to stresses generated by thermal expansion effects. Often engineering failures at high stresses and low numbers of cycling are attributed to low cycle fatigue.[1] In addition to tensile and creep properties and environmental resistance, low cycle fatigue is a critical criterion for design and selection of materials for gas turbines. Yet, neither comparative data for most commonly used alloys are available nor is the fatigue behavior at elevated temperatures sufficiently understood. In this paper, the low cycle fatigue behavior of three alloys, prominently used in gas turbine engines, is presented: HASTELLOY alloy X, INCONEL alloy 617, and HAYNES alloy 230. Alloy X was introduced about 1954 and has been studied over the temperature range of 538°C (1000°F) to 871°C (1600°F), by several investigators[2,3,4,5,6]. All of these works were done under constant but different strain rate conditions. Similarly, alloy 617, introduced about 1974, has been the subject of investigation by Rao et al[7] under various constant strain rate conditions and Burke and Beck[8] under constant frequency. This paper describes for the first time low cycle fatigue results for the 230 alloy and compares these with those for alloy 617 and alloy X, obtained under identical testing conditions at elevated temperatures.

MATERIAL AND PROCEDURE

Results presented in this paper are derived on commercially produced plate materials, [see Table 1 for nominal composition, nominal thickness 16mm (0.625")], in the as-received condition. No subsequent thermal treatment was given to the mill-annealed materials. In this condition the grain sizes for the three alloys were: 230 alloy and alloy X-ASTM 5-5.5 and alloy 617-ASTM 0.5-1. The disparity of grain sizes among the alloys is inevitable, for that is the way the alloys are purposefully made. The coarse-grained structure of alloy 617 contributes to its superior creep strength. Tables 2 through 4 present tensile and creep-rupture data at 760°C (1400°F), 871°C (1600°F) and 982°C (1800°F), respectively. The tensile data were obtained from the material used in this study, while the creep rupture data were compiled from previously conducted work at Haynes International. Table 5 presents dynamic oxidation data for the three alloys for 982°C (1800°F)/-1000-hour test.[9]

Fully reversed (R = -1.0) axial low cycle fatigue testing was carried out at 760°C (1400°F), 871°C (1600°F) and 982°C (1800°F) at f = .33H_z (20cpm), under a strain-controlled mode. The tests used buttonhead, unnotched, low stress ground and polished, smooth bar specimens. The orientation of test specimens was transverse to the rolling direction. Hysteresis loops were periodically plotted generally until the onset of crack initiation. The transition of stable load response to load decay was taken as the number of cycles to crack initiation (Ni); the tests were continued to failure (N_f).

*Presented at the Gas Turbine and Aeroengine Congress and Exposition—June 11-14, 1990—Brussels, Belgium

TABLE 1

NOMINAL COMPOSITIONS OF ALLOYS

Alloy	WT %								
	Ni	Co	Cr	Mo	W	Fe	Al	C	Others
HAYNES® alloy 230	Bal.	5*	22	2	14	3*	0.3	.10	0.02 La
INCONEL® alloy 617	Bal.	12.5	22	9	-	1.5	1.2	.07	0.30 Ti
HASTELLOY® alloy X	Bal.	1.5	22	9	0.6	18.5	-	.10	

* Max.

HAYNES and HASTELLOY are registered trademarks of Haynes International, Inc.
INCONEL is a registered trademark of the INCO Family of Companies.
230 is a trademark of Haynes International, Inc.

TABLE 2

MECHANICAL PROPERTIES

Tensile	760°C (1400°F)		
	230	617	X
0.2% Y.S., MPa (Ksi)	263 (38.1)	196 (28.4)	201 (29.2)
UTS, MPa (Ksi)	586 (85.0)	464 (67.3)	451 (65.4)
% El.	56.5	61.1	59.0
% RA	49.1	45.0	63.7
Creep			
100-Hour 1% Creep Strength, MPa (Ksi)	107 (15.5)	97 (14.0)	93 (13.5)
1000-Hour 1% Creep Strength, MPa (Ksi)	86 (12.5)	68 (9.8)	69 (10.0)
1000-Hour Rupture Strength, MPa (Ksi)	139 (20.2)	148 (21.5)	103 (15.0)

TABLE 3

MECHANICAL PROPERTIES OF 230 ALLOY AND 617 ALLOY ANNEALED

Tensile	871°C (1600°F)		
	230	617	X
0.2% Y.S., MPa (Ksi)	258 (37.4)	214 (31.1)	197 (28.6)
UTS, MPa (Ksi)	445 (64.5)	279 (40.4)	328 (47.5)
% El.	72.9	67.7	64.1
% RA	67.8	62.2	78.4
Creep			
100-Hour 1% Creep Strength, MPa (Ksi)	59 (8.6)	46 (6.7)	46 (6.7)
1000-Hour 1% Creep Strength, MPa (Ksi)	68 (9.8)	32 (4.6)	28 (4.0)
1000-Hour Rupture Strength, MPa (Ksi)	66 (9.5)	62 (9.0)	43 (6.2)

TABLE 4

MECHANICAL PROPERTIES OF 230 ALLOY AND 617 ALLOY ANNEALED

Tensile	982°C (1800°F)		
	230	617	X
0.2% Y.S., MPa (Ksi)	127 (18.4)	130 (18.8)	133 (19.3)
UTS, MPa (Ksi)	247 (35.8)	154 (22.4)	207 (30.0)
% El.	89.2	79.5	68.8
% RA	83.2	65.1	78.6
Creep			
100-Hour 1% Creep Strength, MPa (Ksi)	26 (3.7)	23 (3.3)	19 (2.8)
1000-Hour 1% Creep Strength, MPa (Ksi)	14 (2.0)	-	-
1000-Hour Rupture Strength, MPa (Ksi)	23 (3.3)	26 (3.8)	17 (2.4)

TABLE 5

DYNAMIC OXIDATION DATA: 982°C (1800°F)/1000-Hour

Alloy	Oxidation Attack, μm (mils)		
	Metal Loss	Avg. Metal Affected	Max. Metal Affected
230	20.3 (0.8)	71.1 (2.8)	88.9 (3.5)
X	68.6 (2.7)	142.2 (5.6)	162.6 (6.4)
617	68.6 (2.7)	248.9 (9.8)	271.8 (10.7)

Max. metal affected = Metal loss + max. internal attack

Fuel = 2 parts No. 1 and 1 part No. 2 fuel oil
Fuel: Air = 50:1
Gas Velocity = 0.3 Mach
Samples cycled out every 30 minutes and fan cooled to < 500°F for 2 minutes before reinsertion into hot gas stream.

Fracture and metallographic observations were made on failed samples tested at 982°C (1800°F)-/$\Delta\varepsilon_t$ = 0.4%. Failed samples were cut and mounted longitudinally and repeatedly polished to elicit the nature of secondary cracks.

RESULTS AND DISCUSSION

Fatigue Life

The results of low cycle fatigue tests in terms of total strain range ($\Delta\varepsilon_t$, %) versus cycles to failures (N_f) are plotted on log-log scale in Figures 1 through 3. For design and application purposes this is believed to be the most appropriate way to present the data.[10] The results also are tabulated in Tables 6 through 8. These results show that, for all test conditions, 230 alloy gives the best fatigue life followed by alloy X and alloy 617. At 760°C (1400°F) data for alloy X were not available. It is further observed that, in absolute terms, cycles to crack initiation are far lower in alloy 617. Whether inferior fatigue life of alloy 617 can be attributed to its coarse-grained structure is a hypothetical point since any grain refinement of the structure will substantially alter its creep characteristics. In diffusion creep, the minimum creep rate is generally expressed as follows:

$$\dot{\varepsilon}_{min} \propto (\text{grain size})^{-n}$$

n = 2 or 3, depending on whether volume- or grain-boundary diffusion is the controlling mechanism[11]. Therefore, it may be hypothesized that grain refinement in alloy 617 might result in improved fatigue life, but it will be at the expense of reduced creep strength.

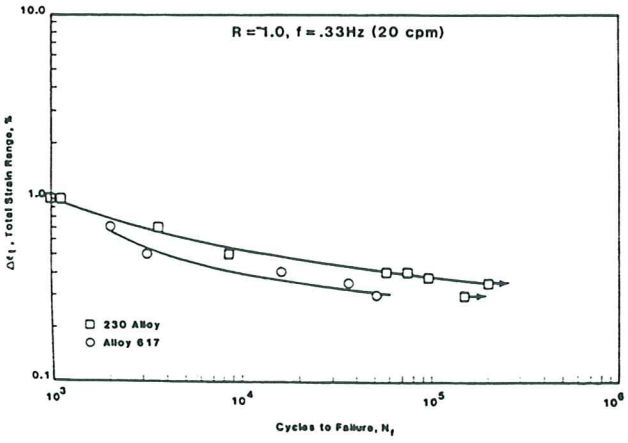

FIG. 1 LOW CYCLE FATIGUE BEHAVIOR AT 760°C (1400°F)

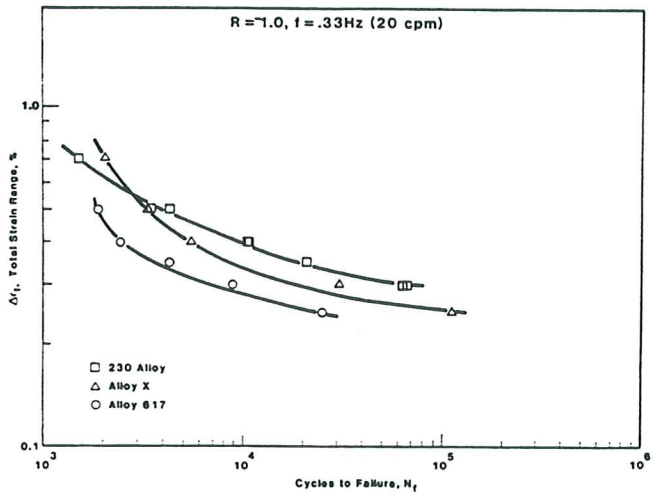

FIG. 2 LOW CYCLE FATIGUE BEHAVIOR AT 871°C (1600°F)

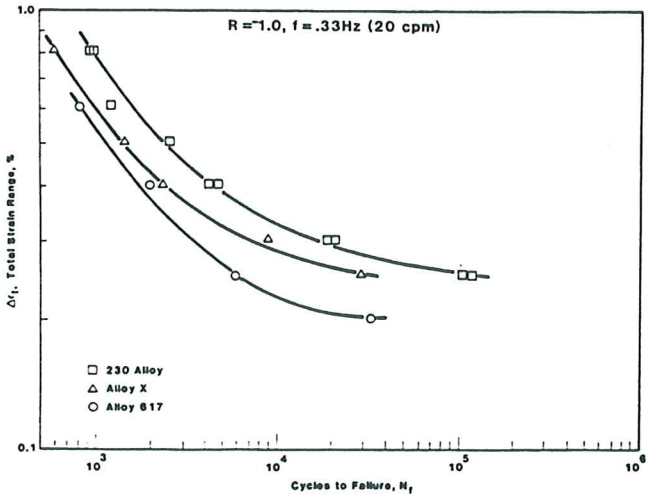

FIG. 3 LOW CYCLE FAILURE BEHAVIOR AT 982°C (1800°F)

Cyclic Hardening and Softening

In cyclic deformation, materials tend to harden or soften until they reach a saturation stress. In fatigue tests, meta-stable alloys are susceptible to accelerated aging, precipitation, etc., accompanied with an increase or degradation of strength. Near independence of N_f on plastic strain in some cases might suggest that strength was the same at all temperatures (Ref. 10, p. 28). Also, cyclic stress/strain data may point to significant microstructural changes. However, in the absence of saturation stress or cyclic stress strain data, the degree of hardening can be ascertained using the modified relationship of Plumbridge et al.(12)

$$H = \frac{\Delta\sigma/2 \text{ at } N_f/2 - \Delta\sigma/2 \text{ at first cycle}}{\Delta\sigma/2 - \Delta\sigma/2 \text{ at first cycle}} \times 100$$

These results are included in Tables 6 through 8. At 760°C (1400°F) alloy 617 shows substantially greater hardening than 230 alloy. For example, for $\Delta\varepsilon_t$ = 0.4%. alloy 617 hardens 83% over 13.5 hours in contrast to 29.4% over 62.9 hours for the latter. It is known that presence of 1.2% Al in alloy 617 causes gamma-prime formation, and cyclic deformation accelerates formation of point defects and thus the diffusion rate. Therefore, it is believed that in alloy 617 the hardening is due to the formation of gamma prime during cyclic deformation. At 982°C (1800°F) alloy X exhibits softening at lower strain ranges, as does alloy 617 at the lowest strain range. These are important findings. The softening may have a deleterious effect during service. This could be caused by environmentally induced initiation of numerous cracks and their subsequent simultaneous propagation or dynamic thermal processes.

TABLE 6

LCF DATA SUMMARY AT 760°C (1400°F)

Total Strain Range %	230 Alloy			Alloy 617		
	Ni Cycles	Nf Cycles	H %	Ni Cycles	Nf Cycles	H %
1.0	870	1097	56.5	-	-	-
.70	3166	3622	35.8	897	2054	-
.50	8153	8490	30.9	2519	3321	91.0
.40	68451	75470	29.4	10285	16160	83.0
.35	91879	97612	-	35736	36333	61.4
.30	-	150000R	-	43962	50360	53.7

R = Runout

TABLE 7

LCF DATA SUMMARY AT 871°C (1600°F)

Total Strain Range %	230 Alloy			Alloy X			Alloy 617		
	Ni Cycles	Nf Cycles	H %	Ni Cycles	Nf Cycles	H %	Ni Cycles	Nf Cycles	H %
.70	1279	1504	27.5	908	2040	-	-	-	-
.50	3939	4299	24.3	2070	3361	-	1490	1894	44.0
.40	9296	10781	16.9	4888	5505	13.3	2026	2461	-
.35	19179	20964	-	-	-	-	3730	4260	29.5
.30	65691	66926	22.3	30308	30698	12.8	6543	8882	24.5
.25	-	200770R	-	102426	111155	5.8	21169	25050	20.7

R = Runout

TABLE 8

LCF DATA SUMMARY AT 982°C (1800°F)

Total Strain Range %	230 Alloy			Alloy X			Alloy 617		
	Ni Cycles	Nf Cycles	H %	Ni Cycles	Nf Cycles	H %	Ni Cycles	Nf Cycles	H %
.80	723	991	7.7	584	1235	.4	-	-	-
.60	818	1218	6.0	-	-	-	447	821	-
.50	1506	2562	10.3	1457	3215	-	-	-	-
.40	3295	4504	4.1	2358	3637	-4.4	994	2000	-
.30	16857	20286	15.4	9000	9321	- .4	-	-	-
.25	111047	112957	11.3	28416	29346	-1.3	4857	5924	9.6
.20	-	-	-	-	-	-	30142	33110	-4.7

Fracture and Metallographic Observations

In Stage I, usually fatigue cracks initiate on some specific slip plane and propagate in the direction of maximum stress. The fracture surface is generally featureless. In stage II, which at high temperatures may correspond to the largest portion of life, cracks advance in a direction perpendicular to the loading axis. In Figure 4, it is easy to identify the location of crack initiation as well as the ductile fracture. Stage II, however, appears very different for 230 alloy and alloy 617. The 230 alloy shows typical fatigue fracture (confirmed by higher magnification SEM examination). The alloy 617 fracture shows radial ridges and striations, but many intergranular facets are also in evidence. This is indicative of transgranular as well as intergranular mixed-mode fracture.

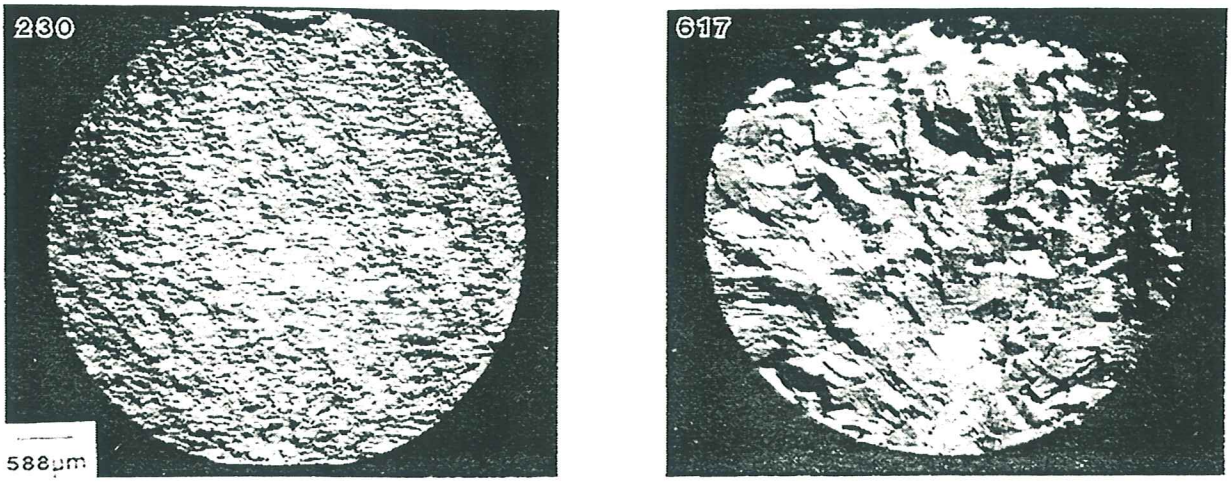

FIG. 4 FRACTURE SURFACES OF FAILED SAMPLES, FATIGUE TESTED AT 982°C (1800°F)/$\Delta\varepsilon_t$ = 0.4%; NOTICE THE CRACK INITIATION AT THE BOTTOM OF PICTURES.

Figure 5 shows the microstructure of 230 alloy in the vicinity of the surface. Repeated polishings failed to reveal the presence of secondary cracks. The microstructure consists of uniformly precipitated $M_{23}C_6$ carbides in the matrix and grain boundaries, plus some discontinuous precipitation at the latter. The secondary cracking and microstructure for alloy X are shown in Figure 6. The cracking apparently initiated at an oxidized grain boundary, propagated part way intergranularly, and subsequently changed to a transgranular mode. The copious secondary precipitation of $M_{23}C_6$, as well as the oxide scale on the surface, are clearly discerible (test duration about three hours). Figure 7.1 shows a composite photograph of an alloy 617 failed specimen, several secondary cracks as well as a secondary fracture are observed. Figure 7.2 shows a secondary crack propagating in a mixed-mode manner. The microstructure shows extensive precipitation of carbides on slip bands near the surface as well as in the matrix. Alloy 617 also exhibited a strong propensity to carbide precipitation on slip bands. Figure 7.3 shows two examples of crack initiation at oxidized grain boundaries. At high temperatures, the environment assumes great importance; the oxidation of grain boundaries and surface oxide spallation enhance crack initiation.[13,14] It appears that oxidation of alloy 617 promotes crack initiation in oxidized grain boundaries. The examination of Figures 7.1 and 7.3 suggests that numerous cracks tend to initiate rather easily in alloy 617. These cracks subsequently propagate simultaneously during Stage II. In Table 5 it is shown that oxidation resistance of alloy X and 617 are appreciably less than that of 230 alloy. This fact seems to have an important bearing on fatigue life of alloy 617, and may explain generally lower N_I/N_f values. In a fine-grained alloy 617 the magnitude of these effects might be greater, since more grain-boundaries at the surface would be available for oxidation. Oxidized boundaries, acting as notches, promote intergranular crack initiation and propagation.

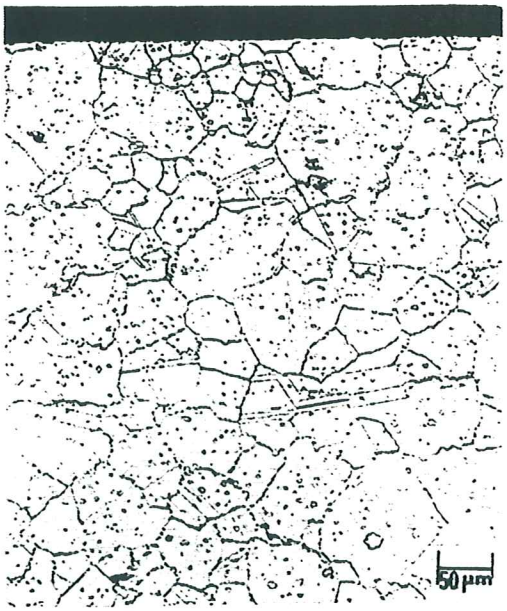

FIG. 5 OPTICAL PHOTOMICROGRAPH OF 230 ALLOY, FATIGUE TESTED AT 982°C (1800°F)/ $\Delta\varepsilon_t$ = .4%; ETCHED.

FIG. 6 OPTICAL PHOTOMICROGRAPH OF ALLOY X, FATIGUE TESTED AT 982°C (1600°F) $\Delta\varepsilon_t$ = .4%, SHOWING SECONDARY CRACKING AND MICROSTRUCTURE; ALSO NOTICE OXIDATION ON THE SURFACE; ETCHED.

FIG. 7.2: OPTICAL PHOTOMICROGRAPH OF ALLOY 617 (SAME SPECIMEN AS IN FIG. 7.1) SHOWING MIXED MODE SECONDARY CRACK PROPAGATION AND MICROSTRUCTURE; ETCHED.

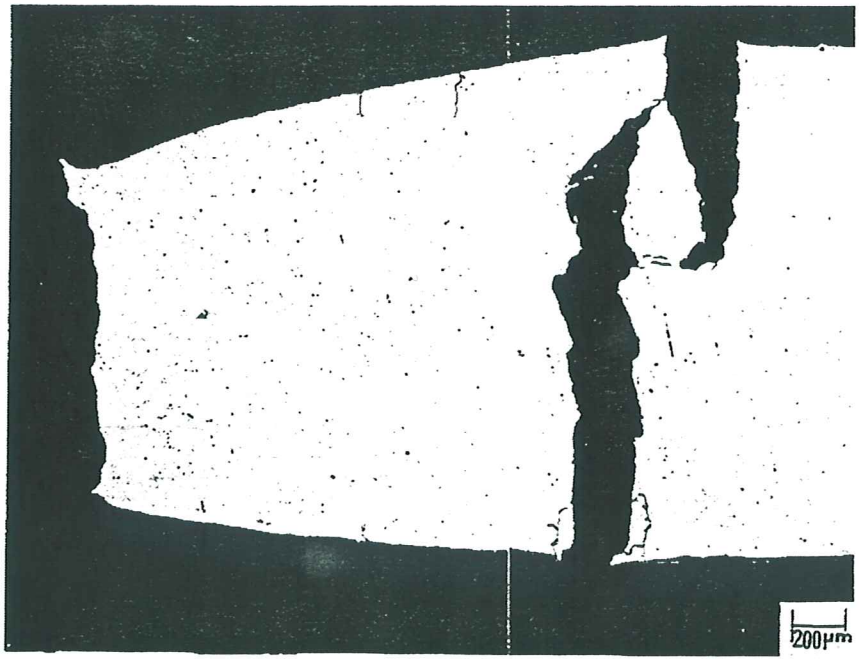

FIG. 7.1 A COMPOSITE PHOTOGRAPH OF ALLOY 617 FAILED SAMPLE, FATIGUE TESTED AT 982°C (1600°F)/$\Delta\varepsilon_t$ = .4%, SHOWING FRACTURE, SECONDARY FRACTURE AND SEVERAL SECONDARY CRACKS; AS-POLISHED.

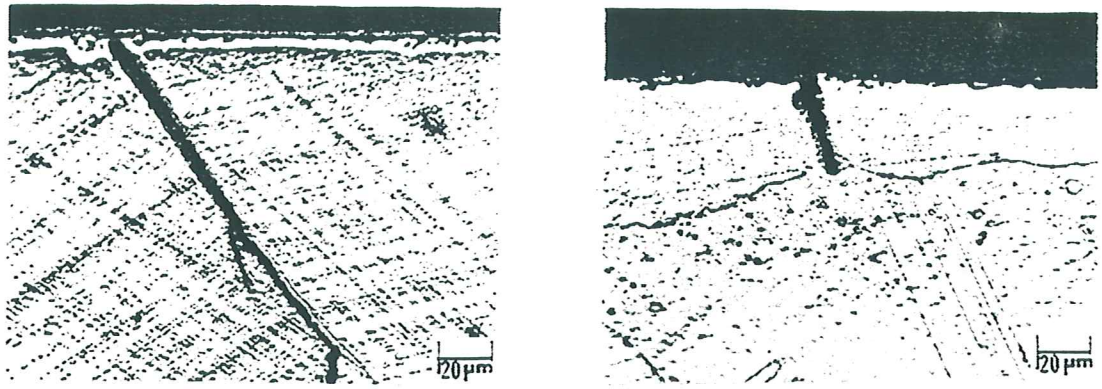

FIG. 7.3 OPTICAL PHOTOMICROGRAPHS OF ALLOY 617 (SAME SPECIMEN AS IN FIG. 7.1) SHOWING OXIDATION ATTACK ALONG GRAIN BOUNDARIES; ETCHED.

SUMMARY

1. Based on the fully revised strain-controlled tests, at 760°C (1400°F), 871°C (1600°F), and 982°C (1800°F), the 230 alloy exhibits the best LCF life followed by alloy X and alloy 617.
2. All of the alloys show a significant degree of cyclic hardening at 760°C (1400°F) and 871°C (1600°F) alloy 617 more so than the other alloys, probably because of gamma prime precipitation. At 982°C (1800°F) however, alloy X, as well as alloy 617, exhibited cyclic softening under certain conditions.
3. Examination of fracture surfaces of failed samples, tested at 982°C (1800°F)/$\Delta\varepsilon_t$ = .40%, showed the propensity of mixed-mode (trans- as well as intergranular) fracture for alloy 617.
4. Numerous secondary cracks were observed in alloy 617. Apparently the crack initiation, often in grain boundaries, is facilitated by oxidation of the alloy. Easy crack initiation and faster intergranular growth appear to be the predominant reasons for inferior low cycle fatigue life for alloy 617.

REFERENCES

1. Dieter, G. E., "Mechanical Metallurgy", McGraw Hill, NY, 1976, p. 411.

2. Jaske, C. E. and Rice, R. C., "Low Cycle Fatigue of Two Austenitic Alloys in Hydrogen Gas and Air at Elevated Temperatures", ASME-MPC Symposium on Creep Fatigue Interaction, New York, 1976, p. 101-128.

3. Jaske, C. E., Rice, R. C., Buchheit, R. D., Roach, D. B. and Porfilio, T. L., "Low Cycle Fatigue of Type 347 Stainless Steel and Hastelloy X in Hydrogen Gas and Air at Elevated Temperatures", NASA-Cr-135022, 1976.

4. Brinkman, C. R., Rittenhouse, P. L., Corwin, W. R., Strizak, J. P., Lystrop, A. and DiStefano, J. R., "Application of Hastelloy X in Gas-Cooled Reactor Systems, ORNL/TM-5405, 1976.

5. Jablonski, D. A., "Fatigue Behavior of Hastelloy X at Elevated Temperatures in Air, Vacuum and Oxygen Environment", Ph.D Thesis, MIT, Cambridge, MA, 1978.

6. Huang, J. S. and Pelloux, R. M., "Low Cycle Fatigue Crack Propagation in HASTELLOY alloy X at 25°C and 760°C", Met Trans., 11A, 1980, p. 899-904.

7. Rao, K. B. S., Schiffers, H., Schuster, H. and Nickel, H., "Influence of Time and Temperature Dependent Processes on Strain Controlled Low Cycle Fatigue Behavior of Alloy 617", Met. Trans. 19A, 1988, p. 359-371.

8. Burke, M. A. and Beck, C. G., "The High Temperature Low Cycle Fatigue of the Nickel Base Alloy IN-617", Met. Trans., 15A, 1984, p. 661-70.

9. Lai, G. Y., Unpublished Research, Haynes International, Inc., 1987.

10. Skelton, R. P., "High Temperature Fatigue", Elsevier, NYU, 1987, p. 28, 60.

11. Poirier, J-P, "Creep of Crystals", Cambridge U.P., Cambridge, 1985, p. 194.

12. Plumbridge, W. J., Dalski, M. E. and Castle, P. J., "High Strain Fatigue of a Type 316 Stainless Steel", Fatigue Eng. Mat. Struct., 3, 1980, p. 177-188.

13. Antolovich, S. D., Bomas, P. and Strudel, J. L., "Low Cycle Fatigue of Rene' 80 as Affected by Prior Exposure", Met. Trans., 10A, 1979, p. 1859-68.

14. Taplin, D.M.R., Tang, N.Y. and Leipholz, H.H.E., "On Fatigue- Creep- Environment Interaction and Feasibility of Fatigue Maps", Sixth Int. Conf. on Fracture, New Delhi, 1984, p. 127-142. Quoted in Ref. (10), p. 201.